FERMILAB-PUB-13-133-E

Search for anomalous quartic $WW\gamma\gamma$ couplings in dielectron and missing energy final states in $p\bar{p}$ collisions at $\sqrt{s} = 1.96$ TeV

V.M. Abazov,[31] B. Abbott,[66] B.S. Acharya,[25] M. Adams,[45] T. Adams,[43] J.P. Agnew,[40] G.D. Alexeev,[31] G. Alkhazov,[35] A. Alton[a],[55] A. Askew,[43] S. Atkins,[53] K. Augsten,[7] C. Avila,[5] F. Badaud,[10] L. Bagby,[44] B. Baldin,[44] D.V. Bandurin,[43] S. Banerjee,[25] E. Barberis,[54] P. Baringer,[52] J.F. Bartlett,[44] U. Bassler,[15] V. Bazterra,[45] A. Bean,[52] M. Begalli,[2] L. Bellantoni,[44] S.B. Beri,[23] G. Bernardi,[14] R. Bernhard,[19] I. Bertram,[38] M. Besançon,[15] R. Beuselinck,[39] P.C. Bhat,[44] S. Bhatia,[57] V. Bhatnagar,[23] G. Blazey,[46] S. Blessing,[43] K. Bloom,[58] A. Boehnlein,[44] D. Boline,[63] E.E. Boos,[33] G. Borissov,[38] A. Brandt,[69] O. Brandt,[20] R. Brock,[56] A. Bross,[44] D. Brown,[14] X.B. Bu,[44] M. Buehler,[44] V. Buescher,[21] V. Bunichev,[33] S. Burdin[b],[38] C.P. Buszello,[37] E. Camacho-Pérez,[28] B.C.K. Casey,[44] H. Castilla-Valdez,[28] S. Caughron,[56] S. Chakrabarti,[63] K.M. Chan,[50] A. Chandra,[71] E. Chapon,[15] G. Chen,[52] S.W. Cho,[27] S. Choi,[27] B. Choudhary,[24] S. Cihangir,[44] D. Claes,[58] J. Clutter,[52] M. Cooke,[44] W.E. Cooper,[44] M. Corcoran,[71] F. Couderc,[15] M.-C. Cousinou,[12] D. Cutts,[68] A. Das,[41] G. Davies,[39] S.J. de Jong,[29,30] E. De La Cruz-Burelo,[28] F. Déliot,[15] R. Demina,[62] D. Denisov,[44] S.P. Denisov,[34] S. Desai,[44] C. Deterre[d],[20] K. DeVaughan,[58] H.T. Diehl,[44] M. Diesburg,[44] P.F. Ding,[40] A. Dominguez,[58] A. Dubey,[24] L.V. Dudko,[33] A. Duperrin,[12] S. Dutt,[23] M. Eads,[46] D. Edmunds,[56] J. Ellison,[42] V.D. Elvira,[44] Y. Enari,[14] H. Evans,[48] V.N. Evdokimov,[34] L. Feng,[46] T. Ferbel,[62] F. Fiedler,[21] F. Filthaut,[29,30] W. Fisher,[56] H.E. Fisk,[44] M. Fortner,[46] H. Fox,[38] S. Fuess,[44] A. Garcia-Bellido,[62] J.A. García-González,[28] V. Gavrilov,[32] W. Geng,[12,56] C.E. Gerber,[45] Y. Gershtein,[59] G. Ginther,[44,62] G. Golovanov,[31] P.D. Grannis,[63] S. Greder,[16] H. Greenlee,[44] G. Grenier,[17] Ph. Gris,[10] J.-F. Grivaz,[13] A. Grohsjean[c],[15] S. Grünendahl,[44] M.W. Grünewald,[26] T. Guillemin,[13] G. Gutierrez,[44] P. Gutierrez,[66] J. Haley,[54] L. Han,[4] K. Harder,[40] A. Harel,[62] J.M. Hauptman,[51] J. Hays,[39] T. Head,[40] T. Hebbeker,[18] D. Hedin,[46] H. Hegab,[67] A.P. Heinson,[42] U. Heintz,[68] C. Hensel,[20] I. Heredia-De La Cruz[d],[28] K. Herner,[44] G. Hesketh[f],[40] M.D. Hildreth,[50] R. Hirosky,[72] T. Hoang,[43] J.D. Hobbs,[63] B. Hoeneisen,[9] J. Hogan,[71] M. Hohlfeld,[21] I. Howley,[69] Z. Hubacek,[7,15] V. Hynek,[7] I. Iashvili,[61] Y. Ilchenko,[70] R. Illingworth,[44] A.S. Ito,[44] S. Jabeen,[68] M. Jaffré,[13] A. Jayasinghe,[66] J. Holzbauer,[57] M.S. Jeong,[27] R. Jesik,[39] P. Jiang,[4] K. Johns,[41] E. Johnson,[56] M. Johnson,[44] A. Jonckheere,[44] P. Jonsson,[39] J. Joshi,[42] A.W. Jung,[44] A. Juste,[36] E. Kajfasz,[12] D. Karmanov,[33] I. Katsanos,[58] R. Kehoe,[70] S. Kermiche,[12] N. Khalatyan,[44] A. Khanov,[67] A. Kharchilava,[61] Y.N. Kharzheev,[31] I. Kiselevich,[32] J.M. Kohli,[23] A.V. Kozelov,[34] J. Kraus,[57] A. Kumar,[61] A. Kupco,[8] T. Kurča,[17] V.A. Kuzmin,[33] S. Lammers,[48] P. Lebrun,[17] H.S. Lee,[27] S.W. Lee,[51] W.M. Lee,[43] X. Lei,[41] J. Lellouch,[14] D. Li,[14] H. Li,[72] L. Li,[42] Q.Z. Li,[44] J.K. Lim,[27] D. Lincoln,[44] J. Linnemann,[56] V.V. Lipaev,[34] R. Lipton,[44] H. Liu,[70] Y. Liu,[4] A. Lobodenko,[35] M. Lokajicek,[8] R. Lopes de Sa,[63] R. Luna-Garcia[g],[28] A.L. Lyon,[44] A.K.A. Maciel,[1] R. Madar,[19] R. Magaña-Villalba,[28] S. Malik,[58] V.L. Malyshev,[31] J. Mansour,[20] J. Martínez-Ortega,[28] R. McCarthy,[63] C.L. McGivern,[40] M.M. Meijer,[29,30] A. Melnitchouk,[44] D. Menezes,[46] P.G. Mercadante,[3] M. Merkin,[33] A. Meyer,[18] J. Meyer[i],[20] F. Miconi,[16] N.K. Mondal,[25] M. Mulhearn,[72] E. Nagy,[12] M. Narain,[68] R. Nayyar,[41] H.A. Neal,[55] J.P. Negret,[5] P. Neustroev,[35] H.T. Nguyen,[72] T. Nunnemann,[22] J. Orduna,[71] N. Osman,[12] J. Osta,[50] A. Pal,[69] N. Parashar,[49] V. Parihar,[68] S.K. Park,[27] R. Partridge[e],[68] N. Parua,[48] A. Patwa[j],[64] B. Penning,[44] M. Perfilov,[33] Y. Peters,[20] K. Petridis,[40] G. Petrillo,[62] P. Pétroff,[13] M.-A. Pleier,[64] V.M. Podstavkov,[44] A.V. Popov,[34] M. Prewitt,[71] D. Price,[48] N. Prokopenko,[34] J. Qian,[55] A. Quadt,[20] B. Quinn,[57] P.N. Ratoff,[38] I. Razumov,[34] I. Ripp-Baudot,[16] F. Rizatdinova,[67] M. Rominsky,[44] A. Ross,[38] C. Royon,[15] P. Rubinov,[44] R. Ruchti,[50] G. Sajot,[11] A. Sánchez-Hernández,[28] M.P. Sanders,[22] A.S. Santos[h],[1] G. Savage,[44] L. Sawyer,[53] T. Scanlon,[39] R.D. Schamberger,[63] Y. Scheglov,[35] H. Schellman,[47] C. Schwanenberger,[40] R. Schwienhorst,[56] J. Sekaric,[52] H. Severini,[66] E. Shabalina,[20] V. Shary,[15] S. Shaw,[56] A.A. Shchukin,[34] V. Simak,[7] P. Skubic,[66] P. Slattery,[62] D. Smirnov,[50] G.R. Snow,[58] J. Snow,[65] S. Snyder,[64] S. Söldner-Rembold,[40] L. Sonnenschein,[18] K. Soustruznik,[6] J. Stark,[11] D.A. Stoyanova,[34] M. Strauss,[66] L. Suter,[40] P. Svoisky,[66] M. Titov,[15] V.V. Tokmenin,[31] Y.-T. Tsai,[62] D. Tsybychev,[63] B. Tuchming,[15] C. Tully,[60] L. Uvarov,[35] S. Uvarov,[35] S. Uzunyan,[46] R. Van Kooten,[48] W.M. van Leeuwen,[29] N. Varelas,[45] E.W. Varnes,[41] I.A. Vasilyev,[34] A.Y. Verkheev,[31] L.S. Vertogradov,[31] M. Verzocchi,[44] M. Vesterinen,[40] D. Vilanova,[15] P. Vokac,[7] H.D. Wahl,[43] M.H.L.S. Wang,[44] J. Warchol,[50] G. Watts,[73] M. Wayne,[50] J. Weichert,[21] L. Welty-Rieger,[47] M.R.J. Williams,[48] G.W. Wilson,[52] M. Wobisch,[53] D.R. Wood,[54] T.R. Wyatt,[40] Y. Xie,[44] R. Yamada,[44] S. Yang,[4] T. Yasuda,[44] Y.A. Yatsunenko,[31] W. Ye,[63] Z. Ye,[44] H. Yin,[44] K. Yip,[64] S.W. Youn,[44] J.M. Yu,[55] J. Zennamo,[61] T.G. Zhao,[40] B. Zhou,[55] J. Zhu,[55] M. Zielinski,[62] D. Zieminska,[48] and L. Zivkovic[14]

(The D0 Collaboration*)

[1]*LAFEX, Centro Brasileiro de Pesquisas Físicas, Rio de Janeiro, Brazil*
[2]*Universidade do Estado do Rio de Janeiro, Rio de Janeiro, Brazil*
[3]*Universidade Federal do ABC, Santo André, Brazil*
[4]*University of Science and Technology of China, Hefei, People's Republic of China*
[5]*Universidad de los Andes, Bogotá, Colombia*
[6]*Charles University, Faculty of Mathematics and Physics, Center for Particle Physics, Prague, Czech Republic*
[7]*Czech Technical University in Prague, Prague, Czech Republic*
[8]*Institute of Physics, Academy of Sciences of the Czech Republic, Prague, Czech Republic*
[9]*Universidad San Francisco de Quito, Quito, Ecuador*
[10]*LPC, Université Blaise Pascal, CNRS/IN2P3, Clermont, France*
[11]*LPSC, Université Joseph Fourier Grenoble 1, CNRS/IN2P3, Institut National Polytechnique de Grenoble, Grenoble, France*
[12]*CPPM, Aix-Marseille Université, CNRS/IN2P3, Marseille, France*
[13]*LAL, Université Paris-Sud, CNRS/IN2P3, Orsay, France*
[14]*LPNHE, Universités Paris VI and VII, CNRS/IN2P3, Paris, France*
[15]*CEA, Irfu, SPP, Saclay, France*
[16]*IPHC, Université de Strasbourg, CNRS/IN2P3, Strasbourg, France*
[17]*IPNL, Université Lyon 1, CNRS/IN2P3, Villeurbanne, France and Université de Lyon, Lyon, France*
[18]*III. Physikalisches Institut A, RWTH Aachen University, Aachen, Germany*
[19]*Physikalisches Institut, Universität Freiburg, Freiburg, Germany*
[20]*II. Physikalisches Institut, Georg-August-Universität Göttingen, Göttingen, Germany*
[21]*Institut für Physik, Universität Mainz, Mainz, Germany*
[22]*Ludwig-Maximilians-Universität München, München, Germany*
[23]*Panjab University, Chandigarh, India*
[24]*Delhi University, Delhi, India*
[25]*Tata Institute of Fundamental Research, Mumbai, India*
[26]*University College Dublin, Dublin, Ireland*
[27]*Korea Detector Laboratory, Korea University, Seoul, Korea*
[28]*CINVESTAV, Mexico City, Mexico*
[29]*Nikhef, Science Park, Amsterdam, the Netherlands*
[30]*Radboud University Nijmegen, Nijmegen, the Netherlands*
[31]*Joint Institute for Nuclear Research, Dubna, Russia*
[32]*Institute for Theoretical and Experimental Physics, Moscow, Russia*
[33]*Moscow State University, Moscow, Russia*
[34]*Institute for High Energy Physics, Protvino, Russia*
[35]*Petersburg Nuclear Physics Institute, St. Petersburg, Russia*
[36]*Institució Catalana de Recerca i Estudis Avançats (ICREA) and Institut de Física d'Altes Energies (IFAE), Barcelona, Spain*
[37]*Uppsala University, Uppsala, Sweden*
[38]*Lancaster University, Lancaster LA1 4YB, United Kingdom*
[39]*Imperial College London, London SW7 2AZ, United Kingdom*
[40]*The University of Manchester, Manchester M13 9PL, United Kingdom*
[41]*University of Arizona, Tucson, Arizona 85721, USA*
[42]*University of California Riverside, Riverside, California 92521, USA*
[43]*Florida State University, Tallahassee, Florida 32306, USA*
[44]*Fermi National Accelerator Laboratory, Batavia, Illinois 60510, USA*
[45]*University of Illinois at Chicago, Chicago, Illinois 60607, USA*
[46]*Northern Illinois University, DeKalb, Illinois 60115, USA*
[47]*Northwestern University, Evanston, Illinois 60208, USA*
[48]*Indiana University, Bloomington, Indiana 47405, USA*
[49]*Purdue University Calumet, Hammond, Indiana 46323, USA*
[50]*University of Notre Dame, Notre Dame, Indiana 46556, USA*
[51]*Iowa State University, Ames, Iowa 50011, USA*
[52]*University of Kansas, Lawrence, Kansas 66045, USA*
[53]*Louisiana Tech University, Ruston, Louisiana 71272, USA*
[54]*Northeastern University, Boston, Massachusetts 02115, USA*
[55]*University of Michigan, Ann Arbor, Michigan 48109, USA*
[56]*Michigan State University, East Lansing, Michigan 48824, USA*
[57]*University of Mississippi, University, Mississippi 38677, USA*
[58]*University of Nebraska, Lincoln, Nebraska 68588, USA*
[59]*Rutgers University, Piscataway, New Jersey 08855, USA*
[60]*Princeton University, Princeton, New Jersey 08544, USA*

[61] State University of New York, Buffalo, New York 14260, USA
[62] University of Rochester, Rochester, New York 14627, USA
[63] State University of New York, Stony Brook, New York 11794, USA
[64] Brookhaven National Laboratory, Upton, New York 11973, USA
[65] Langston University, Langston, Oklahoma 73050, USA
[66] University of Oklahoma, Norman, Oklahoma 73019, USA
[67] Oklahoma State University, Stillwater, Oklahoma 74078, USA
[68] Brown University, Providence, Rhode Island 02912, USA
[69] University of Texas, Arlington, Texas 76019, USA
[70] Southern Methodist University, Dallas, Texas 75275, USA
[71] Rice University, Houston, Texas 77005, USA
[72] University of Virginia, Charlottesville, Virginia 22904, USA
[73] University of Washington, Seattle, Washington 98195, USA

(Dated: May 6, 2013)

We present a search for anomalous components of the quartic gauge boson coupling $WW\gamma\gamma$ in events with an electron, a positron and missing transverse energy. The analyzed data correspond to $9.7\,\mathrm{fb}^{-1}$ of integrated luminosity collected by the D0 detector in $p\bar{p}$ collisions at $\sqrt{s} = 1.96\,\mathrm{TeV}$. The presence of anomalous quartic gauge couplings would manifest itself as an excess of boosted WW events. No such excess is found in the data, and we set the most stringent limits to date on the anomalous coupling parameters a_0^W and a_C^W. When a form factor with $\Lambda_{\mathrm{cutoff}} = 0.5\,\mathrm{TeV}$ is used, the observed upper limits at 95% C.L. are $|a_0^W/\Lambda^2| < 0.0025\ \mathrm{GeV}^{-2}$ and $|a_C^W/\Lambda^2| < 0.0092\ \mathrm{GeV}^{-2}$.

PACS numbers: 14.70.Fm,12.60.Cn,13.85.Qk

I. INTRODUCTION

In the standard model (SM) of particle physics, the couplings of fermions and gauge bosons are constrained by the gauge symmetries of the Lagrangian. The non-abelian gauge nature of the SM predicts the existence of trilinear (VVV) and quartic ($VVVV$) gauge couplings ($V = \gamma, W, Z$). These include quartic couplings $WW\gamma\gamma$ between W bosons and photons that can be probed directly at hadron colliders [1–3], but that are too small to be observed at the Tevatron, as will be shown later. Quartic couplings provide a window on electroweak symmetry breaking [4, 5] and can be probed by the measurement of W boson pair production via two photon exchange.

Quartic couplings also allow for probing new physics that couples to electroweak bosons. As an example, the contribution of virtual heavy particles beyond the SM might manifest itself as a modification of the quartic couplings between W bosons and photons [6–8]. Observing the resulting anomalous couplings from such processes could be the first evidence of new physics in the electroweak sector of the SM.

In this paper, we will focus on the search for $WW\gamma\gamma$ anomalous quartic gauge couplings (AQGCs) using data collected by the D0 experiment at the Fermilab $p\bar{p}$ Tevatron Collider, in events with an electron, a positron and missing transverse energy. The main production diagrams are shown in Fig. 1. Pairs of W bosons are produced via photon exchange, where the photons are directly radiated from the colliding proton and antiproton. Triple gauge couplings $WW\gamma$ are assumed to be at their SM values (deviations from these values have been constrained by the D0 Collaboration [9] and others [10–13]).

The parameterization of the AQGCs is based on Ref. [14], and only the lowest dimension operators that have the correct Lorentz invariant structure and fulfill $SU(2)_C$ custodial symmetry [15] are considered. Such operators involving two W bosons and two photons are of dimension six:

$$\begin{aligned} \mathcal{L}_6^0 &= \frac{-e^2}{8}\frac{a_0^W}{\Lambda^2} F_{\mu\nu}F^{\mu\nu}W^{+\alpha}W^-_{\alpha} \\ \mathcal{L}_6^C &= \frac{-e^2}{16}\frac{a_C^W}{\Lambda^2} F_{\mu\alpha}F^{\mu\beta}(W^{+\alpha}W^-_{\beta} + W^{-\alpha}W^+_{\beta}), \end{aligned} \quad (1)$$

where $F^{\mu\nu}$ is the electromagnetic field strength tensor and $W^{\pm}_{\alpha}$ is the $W^{\pm}$ boson field. a_0^W and a_C^W are the usual notation for the parametrized quartic coupling constants, where a non-zero a_0^W could be due to an exchange of a heavy neutral scalar, while heavy charged fermions would contribute to both a_0^W and a_C^W. The new scale Λ is introduced so that the Lagrangian density has the correct dimension of four and is interpreted as the typical mass scale of new physics. The current best 95% C.L. limits on these anomalous parameters come from the OPAL Collaboration from measurement of $WW\gamma$, $q\bar{q}\gamma\gamma$ and $\nu\bar{\nu}\gamma\gamma$ production [16] at the CERN LEP Collider:

*with visitors from [a] Augustana College, Sioux Falls, SD, USA, [b] The University of Liverpool, Liverpool, UK, [c] DESY, Hamburg, Germany, [d] Universidad Michoacana de San Nicolas de Hidalgo, Morelia, Mexico [e] SLAC, Menlo Park, CA, USA, [f] University College London, London, UK, [g] Centro de Investigacion en Computacion - IPN, Mexico City, Mexico, [h] Universidade Estadual Paulista, São Paulo, Brazil, [i] Karlsruher Institut für Technologie (KIT) - Steinbuch Centre for Computing (SCC) and [j] Office of Science, U.S. Department of Energy, Washington, D.C. 20585, USA.

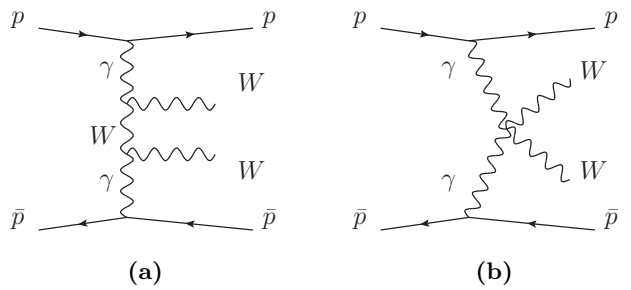

FIG. 1: Diagrams contributing to W boson pair production via photon exchange, with (a) triple $WW\gamma$ and (b) quartic $WW\gamma\gamma$ couplings.

.

$$\begin{aligned} -0.020\,\mathrm{GeV}^{-2} < \ a_0^W/\Lambda^2 \ < 0.020\,\mathrm{GeV}^{-2} \\ -0.052\,\mathrm{GeV}^{-2} < \ a_C^W/\Lambda^2 \ < 0.037\,\mathrm{GeV}^{-2}. \end{aligned} \tag{2}$$

The $p\bar{p} \to p\bar{p}\,W^+W^-$ cross section via photon exchange rises quickly at high energies when the anomalous coupling parameters are non-zero, and manifests itself in particular with the production of boosted W boson pairs. In the SM, the $\gamma\gamma \to WW$ cross section is constant in the high-energy limit due to the cancellation between the relevant diagrams. When the new quartic terms are added, the cancellation does not hold and the cross section will grow to violate unitarity at high energies. This increase of the cross section can be regularized with a form factor that reduces the values of a_0^W and a_C^W at high energy while not modifying them at lower energies. Following a standard approach, we introduce the following form factor [6]:

$$a_i^W \to \frac{a_i^W}{(1 + M_{\gamma\gamma}^2/\Lambda_{\mathrm{cutoff}}^2)^2}, \tag{3}$$

where $M_{\gamma\gamma}$ is the invariant mass of the two photons, and $\Lambda_{\mathrm{cutoff}}$ is chosen to be either 0.5 or 1 TeV, following the prescription of, e.g., Ref. [6]. In the following, we provide limits on anomalous couplings with and without form factors.

II. DATA AND MONTE CARLO SAMPLES

The full Run II set of data recorded by the D0 detector is considered in this analysis, representing $9.7\,\mathrm{fb}^{-1}$ of $p\bar{p}$ collisions at $\sqrt{s} = 1.96\,\mathrm{TeV}$ delivered by the Tevatron between 2002 and 2011, after the relevant data quality requirements are invoked. The D0 detector used for Run II is described in detail in Ref. [17]. The innermost part of the detector is composed of a central tracking system with a silicon microstrip tracker (SMT) and a central fiber tracker embedded within a 2 T solenoidal magnet. The tracking system is surrounded by a central preshower detector and a liquid-argon/uranium calorimeter with electromagnetic, fine, and coarse hadronic sections. The central calorimeter (CC) covers pseudorapidity [18] $|\eta_d| \lesssim 1.1$. Two end calorimeters (EC) extend the coverage to $1.4 \lesssim |\eta_d| \lesssim 4.2$. Energy sampling in the region between the ECs and CC is improved by the addition of scintillating tiles. A muon spectrometer, with pseudorapidity coverage of $|\eta_d| \lesssim 2$, resides outside the calorimetry and is comprised of drift tubes, scintillation counters, and toroidal magnets. Trigger decisions are based on information from the tracking detectors, calorimeters, and muon spectrometer. Details on the reconstruction and identification criteria for electrons, jets, and missing transverse energy, $\not\!\!E_T$, can be found elsewhere [19]. In this paper we call both electrons and positrons "electrons," with the charge of the particle determined from the curvature of the associated tracks in the central tracking system.

The background where, like the signal, the proton and the antiproton are intact in the final state, originates from photon exchange and double pomeron exchange (DPE) processes [20]. Both these backgrounds and the AQGC signals are modeled using the FPMC [21] generator, followed by a detailed GEANT3-based [22] simulation of the D0 detector. Data from random beam crossings are overlaid on the MC events to account for detector noise and additional $p\bar{p}$ interactions. The predictions of the FPMC generator, which are made assuming that the proton and antiproton are left intact after the interaction, are consistent with those of the LPAIR [23] generator, which in turn are consistent with the measurement of the cross section for exclusive e^+e^- production by the CDF Collaboration [24].

Diffractive and photon exchange backgrounds to this search are exclusive e^+e^- and $\tau^+\tau^-$ production through t-channel photon exchange (Drell-Yan) and inclusive W^+W^-, e^+e^-, and $\tau^+\tau^-$ production through DPE.

Since the outgoing intact proton and antiproton are not detected in this measurement, we also need to consider non-diffractive backgrounds. These backgrounds are Z/γ^*+jets, $t\bar{t}$ and diboson (W^+W^-, $W^\pm Z$ and ZZ) production, and processes in which jets are misidentified as electrons: W+jets and multijet production. The simulated samples used to model them are identical to those described in Ref. [19]. All of these backgrounds, except multijet production, are modeled using the PYTHIA [25] or ALPGEN [26] generator, with PYTHIA providing showering and hadronization in the latter case, using the CTEQ6L1 [27] parton distribution functions (PDFs). The multijet background is determined from the data by inverting some electron selection criteria, as described in Ref. [19].

Single diffractive (SD) processes, for which either the incoming proton or antiproton is intact after the interaction while the other is destroyed, have similar features to non-diffractive (ND) processes in the direction of the broken proton or antiproton, contrary to DPE processes where both the proton and antiproton are intact. Since

the cross section ratio of SD to ND processes is about (2–3)%, which is below the uncertainty on cross sections of ND processes cross sections, the contribution of SD processes is neglected in this analysis.

The selection of data events is similar but more strict than the search for the Higgs boson in the $H \to W^+W^- \to e^+\nu e^-\bar{\nu}$ channel that is described in detail elsewhere [19], which includes the same trigger approach with no explicit requirement. A preselection is applied to the data by requiring two high-transverse momentum (high-p_T) electrons with opposite charge. The leading- and trailing-p_T electrons are required to satisfy $p_T^{e1} > 15\,\text{GeV}$ and $p_T^{e2} > 10\,\text{GeV}$, and their invariant mass is required to be $M_{ee} > 15\,\text{GeV}$. In addition, these electrons are required to be within the acceptance of the calorimeter ($|\eta_d| < 1.1$ or $1.5 < |\eta_d| < 2.5$ [18]), with at least one electron required to be in the central part of the calorimeter ($|\eta_d| < 1.1$). The only difference from the event selection in the Higgs boson search is that we veto events with at least one jet with $p_T > 20$ GeV, $|\eta_d| < 2.4$, and matched to at least two tracks associated with the $p\bar{p}$ interaction vertex. The inclusive cross section for exclusive W boson pair production through photon exchange in the SM at $\sqrt{s} = 2\,\text{TeV}$ is $\sigma(p\bar{p} \to p\bar{p}WW) = 3\,\text{fb}$, but after the preselection only 0.1 event is expected from this process, unless it is enhanced by AQGCs.

To correct for any possible mismodeling of the lepton reconstruction and trigger efficiencies, and to reduce the impact of the luminosity uncertainty, scale factors are applied to the Monte Carlo (MC) samples at the preselection stage to match the data. The Z boson mass peak region in the data and MC samples after the preselection is used to determine normalization factors. Their differences from unity are found to be consistent with the luminosity uncertainty of 6.1% [28]. The p_T distribution of Z bosons is weighted to match the distribution observed in data [29], taking into account its dependence on the number of reconstructed jets. The p_T distribution of W bosons is weighted to match the measured Z boson p_T spectrum, corrected for the differences between the W and Z p_T spectra predicted in NNLO QCD [30]. The distribution of the p_T of the leading electron after the preselection is shown in Fig. 2(a).

Following the same strategy as described in Ref. [19], boosted decision trees (BDT) are used to reject the large Z/γ^*+jets background, that is dominant after the preselection. The input variables to this "selection BDT" are kinematic quantities, including the electron momenta, the azimuthal opening angle between the two electrons, $\not\!\!E_T$, variables that take into account both $\not\!\!E_T$ and its direction relative to each electron, and observables that differentiate between real and misreconstructed $\not\!\!E_T$. The cut on the selection BDT, which defines the final selection, is chosen such that the contributions of the Z/γ^*+jets, W+jets, and diboson backgrounds are of comparable magnitude. The distribution of the single most discriminating variable, the transverse mass of the $\not\!\!E_T$ and the dielectron pair ($M_T(ee, \not\!\!E_T) = \sqrt{2 \cdot p_T^{ee} \cdot \not\!\!E_T \cdot [1 - \cos\Delta\phi(ee, \not\!\!E_T)]}$), after the final selection is shown in Fig. 2(b). The expected and observed numbers of events after the preselection and the final selection are given in Table I.

A final BDT is trained to separate the AQGC signal from all the other backgrounds. The same BDT is used in the study of both parameters a_0^W and a_C^W, which feature identical kinematic characteristics. This BDT relies on the input variables of the selection BDT, complemented with additional variables characterizing the electron reconstruction quality to discriminate against the instrumental backgrounds (multijet and W+jets production). The distribution of the final BDT output is shown in Fig. 2(c) and demonstrates the good agreement between the data and the background expectation.

III. SYSTEMATIC UNCERTAINTIES

Systematic uncertainties are estimated for the signal and for each background process. They can affect only the normalization or both the normalization and the shape of the final discriminant.

Sources of systematic uncertainty that affect only the normalization arise from the uncertainties on the theoretical cross sections of Z+jets (6%), W+jets (16%), diboson (6%), and $t\bar{t}$ (7%) processes; the multijet normalization (30%); and the modeling of the $\not\!\!E_T$ for the Z+jets background (5%). The diffractive backgrounds have been assigned a 100% uncertainty on their cross sections due to the large uncertainties on the gluon density (for processes induced by pomeron exchange; the uncertainty on the gluon density inside the pomeron can reach 40%, translating into an uncertainty of a factor up to 2 on the cross section) and on the proton dissociation (for processes induced by photon exchange). For the latter process, a 20% uncertainty has been assigned to the signal theoretical cross section.

The sources of systematic uncertainty that also affect the shape of the final discriminant distribution are quoted here as average fractional uncertainty across bins of the final discriminant distribution for all backgrounds: jet energy scale (4%), jet resolution (0.5%), $\not\!\!E_T$ modeling (4%), jet identification (2%), jet association to the hard-scatter primary $p\bar{p}$ interaction vertex (2%), and W+jets modeling (10%). The systematic uncertainties due to the modeling of the $p_T(WW)$ and the $\Delta\phi$ between the leptons, and the p_T of the vector boson from the W+jets and Z+jets production (see Ref. [19]) are less than 1% and taken into account.

IV. RESULTS

The data are found to be in good agreement with the background-only prediction, and upper limits are set on the anomalous parameters a_0^W and a_C^W. The modified frequentist CL_s method [31] is employed to set limits on the

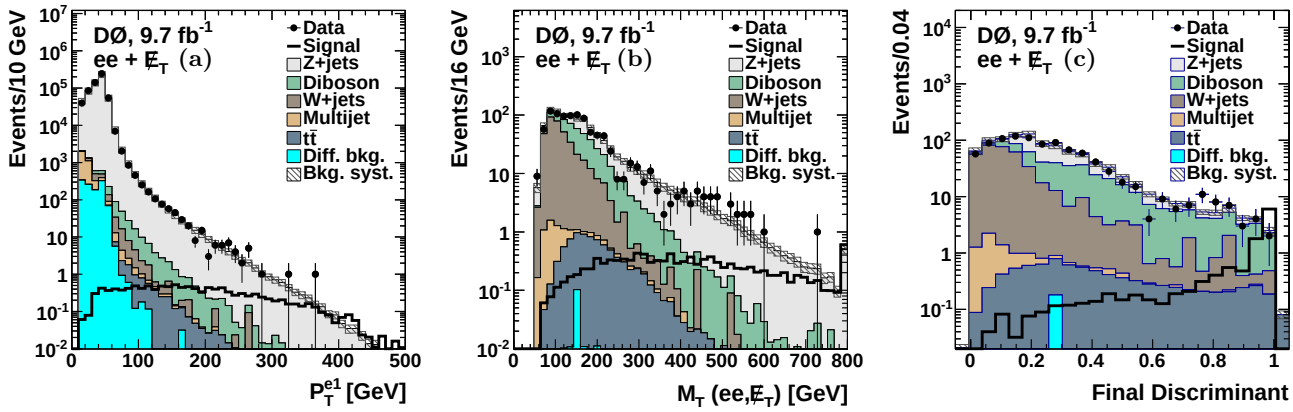

FIG. 2: [color online] The (a) leading electron p_T at the preselection level, (b) the transverse mass of the $\not\!\!E_T$ and the two electrons after the final selection, and (c) the output of the final BDT discriminant after the final selection. In (a) and (b), the last bin includes all events above the upper bound of the histogram. The hatched bands show the total systematic uncertainty on the background prediction, and the signal distributions are those expected for $a_0^W/\Lambda^2 = 5 \times 10^{-4}\,\mathrm{GeV}^{-2}$ and no form factor.

TABLE I: Observed and expected numbers of events after the preselection and the final selection for data, signal ($a_0^W/\Lambda^2 = 5 \times 10^{-4}\,\mathrm{GeV}^{-2}$ and no form factor), and the different backgrounds considered in the analysis ("Diff" stands for the diffractive backgrounds).

	Data	Total background	Signal	$Z/\gamma^\star \to ee$	$Z/\gamma^\star \to \tau\tau$	$t\bar{t}$	W+jets	Diboson	Multijet	Diff.
Preselection:	572700	576576 ± 11532	12.2	566800	4726	15	623	517	2716	1180
Final selection:	946	983 ± 108	11.6	291	22	8	370	287	5.4	0.2

AQGCs, where the test statistic is a log-likelihood ratio (LLR) for the background-only and signal+background hypotheses. The LLR is obtained by summing the LLR values of the bins of the final BDT output. In the LLR calculation, the signal and background rates are functions of the systematic uncertainties that are taken into account as nuisance parameters with Gaussian priors. Their degrading effect is reduced by fitting the expected contributions to the data by maximizing the profile likelihood function for the background-only and signal+background hypotheses separately, appropriately taking into account all correlations between the systematic uncertainties [32].

The 95% C.L. allowed ranges for the anomalous parameter a_0^W (a_C^W) can be found in Table II (III), assuming a_C^W (a_0^W) is zero. The limits are quoted both without a form factor and for a form factor with $\Lambda_{\mathrm{cutoff}} = 1$ or 0.5 TeV (as advised, e.g., in Ref. [6]). The two-parameter limits are shown in Fig. 3 for different assumptions about the signal, namely if no form factor is used and if a form factor is used with $\Lambda_{\mathrm{cutoff}} = 1$ or 0.5 TeV. The two-parameter 68% C.L. (95% C.L.) limits define the range of values of the anomalous coupling parameters for which the theoretical cross section is lower than the upper 68% C.L. (95% C.L.) limit on the signal cross section, obtained in the single parameter limits. The effect of the presence of a Higgs boson with $M_H = 125$ GeV is not accounted for, but is expected to contribute less than 4 events after the final selection, having kinematic distributions distinct from signal, and to broaden the allowed ranges for the anomalous parameters by a negligible amount.

V. CONCLUSION

We have searched for anomalous $WW\gamma\gamma$ quartic gauge boson couplings by analyzing 9.7 fb^{-1} of integrated luminosity in the $W^+W^- \to e^+\nu e^-\bar{\nu}$ final state using the D0 detector. No excess above the background expectation has been found. When a form factor with $\Lambda_{\mathrm{cutoff}} = 0.5$ TeV is used, the observed upper limits at 95% C.L. are $|a_0^W/\Lambda^2| < 0.0025\,\mathrm{GeV}^{-2}$ and $|a_C^W/\Lambda^2| < 0.0092\,\mathrm{GeV}^{-2}$. These are a factor 4 to 8 more stringent constraints on a_0^W and a_C^W than the previous limits [16], and the only published limits to date from a hadron collider.

We thank the staffs at Fermilab and collaborating institutions, and acknowledge support from the DOE and NSF (USA); CEA and CNRS/IN2P3 (France); MON, NRC KI and RFBR (Russia); CNPq, FAPERJ, FAPESP and FUNDUNESP (Brazil); DAE and DST (India); Colciencias (Colombia); CONACyT (Mexico); NRF (Korea); FOM (The Netherlands); STFC and the Royal Society (United Kingdom); MSMT and GACR (Czech Republic); BMBF and DFG (Germany); SFI (Ireland); The Swedish Research Council (Sweden); and CAS and CNSF (China).

TABLE II: Expected and observed 95% C.L upper limits on $|a_0^W/\Lambda^2|$, assuming a_C^W is zero and for different assumptions about the form factor.

Cutoff	Expected upper limit [GeV^{-2}]	Observed upper limit [GeV^{-2}]
No form factor	0.00043	0.00043
$\Lambda_{\rm cutoff} = 1$ TeV	0.00092	0.00089
$\Lambda_{\rm cutoff} = 0.5$ TeV	0.0025	0.0025

TABLE III: Expected and observed 95% C.L upper limits on $|a_C^W/\Lambda^2|$, assuming a_0^W is zero and for different assumptions about the form factor.

Cutoff	Expected upper limit [GeV^{-2}]	Observed upper limit [GeV^{-2}]
No form factor	0.0016	0.0015
$\Lambda_{\rm cutoff} = 1$ TeV	0.0033	0.0033
$\Lambda_{\rm cutoff} = 0.5$ TeV	0.0090	0.0092

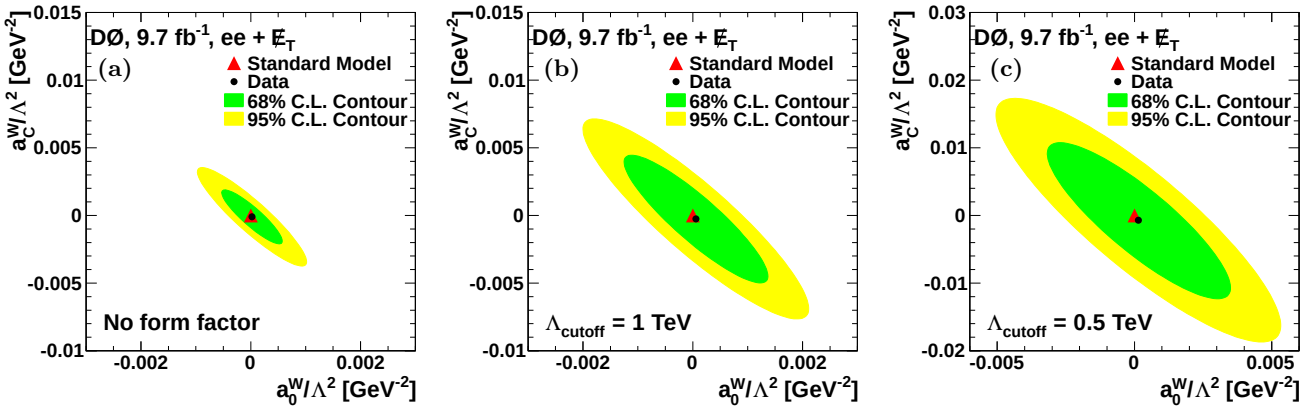

FIG. 3: [color online] Two-parameter 68% and 95% C.L limits with different assumptions about the signal: (a) no form factor, or a form factor with (b) $\Lambda_{\rm cutoff} = 1$ or (c) 0.5 TeV.

[1] E. Chapon, O. Kepka, and C. Royon, Phys. Rev. D **81**, 074003 (2010).
[2] O. Kepka, and C. Royon, Phys. Rev. D **78**, 073005 (2008).
[3] J. de Favereau de Jeneret *et al.*, arXiv:0908.2020 [hep-ph].
[4] P. J. Dervan, A. Signer, W. J. Stirling, and A. Werthenbach, J. Phys. G **26**, 607 (2000).
[5] W. J. Stirling, A. Werthenbach, Eur. Phys. J. C **14**, 103 (2000).
[6] O. J. P. Eboli, M. C. Gonzales-Garcia, S. M. Lietti, and S. F. Novaes, Phys. Rev. D **63**, 075008 (2001).
[7] G. Cvetic and B. Kogerler, Nucl. Phys. **B363**, 401 (1991).
[8] A. Hill, J.J. van der Bij, Phys. Rev. D **36**, 3463 (1987).
[9] V. M. Abazov *et al.* [D0 Collaboration], Phys. Lett. B **718**, 451 (2012).
[10] T. Aaltonen *et al.* [CDF Collaboration], Phys. Rev. Lett. **104**, 201801 (2010).
[11] S. Schael *et al.* [ALEPH Collaboration], Phys. Lett. B **614**, 7 (2005); G. Abbiendi *et al.* [OPAL Collaboration], Eur. Phys. J. C **33**, 463 (2004); P. Achard *et al.* [L3 Collaboration], Phys. Lett. B **586**, 151 (2004); J. Abdallah *et al.* [DELPHI Collaboration], Eur. Phys. J. C **66**, 35 (2010).
[12] G. Aad *et al.* [ATLAS Collaboration], Phys. Lett. B **717**, 49 (2012); G. Aad *et al.* [ATLAS Collaboration], Phys. Lett. B **712**, 289 (2012); G. Aad *et al.* [ATLAS Collaboration], arXiv:1210.2979 [hep-ex]; G. Aad *et al.* [ATLAS Collaboration], arXiv:1302.1283 [hep-ex].
[13] S. Chatrchyan *et al.* [CMS Collaboration], Phys. Lett. B **699**, 25 (2011); S. Chatrchyan *et al.* [CMS Collaboration], Phys. Lett. B **701**, 535 (2011); S. Chatrchyan *et al.* [CMS Collaboration], Eur. Phys. J. C **73**, 2283 (2013).
[14] G. Belanger and F. Boudjema, Phys. Lett. B **288**, 210 (1992). In the present study, the a_0^Z and a_C^Z parameters are assumed to be zero.
[15] R. A. Diaz and R. Martinez, Rev. Mex. Fis. **47**, 489 (2001).

[16] G. Abbiendi *et al.* [OPAL Collaboration], Phys. Rev. D **70**, 032005 (2004).

[17] V. M. Abazov *et al.* [D0 Collaboration], Nucl. Instrum. Meth. Phys. Res. A **565**, 463 (2006); M. Abolins *et al.*, Nucl. Instrum. Meth. Phys. Res. A **584**, 75 (2008); R. Angstadt *et al.*, Nucl. Instrum. Meth. Phys. Res. A **622**, 298 (2010).

[18] The pseudorapidity is defined as $\eta = -\ln(\tan\theta/2)$, where θ is the polar angle relative to the proton beam direction. η_d is the detector pseudorapidity, calculated using the position of the calorimeter cluster with respect to the center of the detector.

[19] V. M. Abazov *et al.* [D0 Collaboration], to be published in Phys. Rev. D, arXiv:1301.1243 [hep-ex] (2013).

[20] M. Boonekamp, F. Chevallier, C. Royon, and L. Schoeffel, Acta Phys. Polon. B **40**, 2239 (2009).

[21] Forward Physics Monte Carlo (FPMC): M. Boonekamp, V. Juránek, O. Kepka, and C. Royon, in Proceedings of the Workshop of the Implications of HERA for LHC Physics, Hamburg-Geneva, 2006-2008, p. 758; M. Boonekamp *et al.*, arXiv:1102.2531v1 [hep-ph], http://cern.ch/fpmc.

[22] R. Brun and F. Carminati, CERN Program Library Long Writeup W5013, 1993 (unpublished).

[23] J. Vermaseren, Nucl. Phys. **B229**, 347 (1983).

[24] T. Aaltonen *et al.* [CDF Collaboration], Phys. Rev. Lett. **108**, 081801 (2012).

[25] T. Sjöstrand, S. Mrenna, and P. Skands, J. High Energy Phys. **05**, 026 (2006); we use versions 6.319 and 6.413.

[26] M. L. Mangano *et al.*, J. High Energy Phys. **07**, 001 (2003); we use version 2.11.

[27] J. Pumplin *et al.*, J. High Energy Phys. **07**, 12 (2002).

[28] T. Andeen *et al.* [D0 Collaboration], FERMILAB-TM-2365.

[29] V. M. Abazov *et al.* [D0 Collaboration], Phys. Rev. Lett. **100**, 102002 (2008).

[30] K. Melnikov and F. Petriello, Phys. Rev. D **74**, 114017 (2006).

[31] T. Junk, Nucl. Instrum. Meth. Phys. Res. A **434**, 435 (1999); A. Read, J. Phys. G **28**, 2693 (2002).

[32] W. Fisher, FERMILAB-TM-2386-E (2006).